

Validation of polymer-based screen-printed textile electrodes for surface EMG detection

*Original*

Validation of polymer-based screen-printed textile electrodes for surface EMG detection / Pani, D; Achilli, A; Spanu, A; Bonfiglio, A; Gazzoni, M; Botter, A. - In: IEEE TRANSACTIONS ON NEURAL SYSTEMS AND REHABILITATION ENGINEERING. - ISSN 1534-4320. - STAMPA. - 27:7(2019), pp. 1370-1377. [10.1109/TNSRE.2019.2916397]

*Availability:*

This version is available at: 11583/2734805 since: 2019-10-16T16:08:46Z

*Publisher:*

IEEE Computer Society

*Published*

DOI:10.1109/TNSRE.2019.2916397

*Terms of use:*

openAccess

This article is made available under terms and conditions as specified in the corresponding bibliographic description in the repository

*Publisher copyright*

IEEE postprint/Author's Accepted Manuscript

©2019 IEEE. Personal use of this material is permitted. Permission from IEEE must be obtained for all other uses, in any current or future media, including reprinting/republishing this material for advertising or promotional purposes, creating new collecting works, for resale or lists, or reuse of any copyrighted component of this work in other works.

(Article begins on next page)

# Validation of Polymer-Based Screen-Printed Textile Electrodes for Surface EMG Detection

D. Pani<sup>1</sup>, A. Achilli<sup>1</sup>, A. Spanu, A. Bonfiglio, M. Gazzoni<sup>2</sup>, and A. Botter<sup>2</sup>

**Abstract**—In recent years, the variety of textile electrodes developed for electrophysiological signal detection has increased rapidly. Among the applications that could benefit from this advancement, those based on surface electromyography (sEMG) are particularly relevant in rehabilitation, training, and muscle function assessment. In this work, we validate the performance of polymer-based screen-printed textile electrodes for sEMG signal detection. We obtained these electrodes by depositing poly-3,4-ethylenedioxythiophene doped with poly(styrene sulfonate) (PEDOT:PSS) onto cotton fabric, and then selectively changing the physical properties of the textile substrate. The manufacturing costs are low and this process meets the requirements of textile-industry production lines. The validation of these electrodes was based on their functional and electrical characteristics, assessed for two different electrode sizes and three skin-interface conditions (dry, solid hydrogel, or saline solution), and compared to those of conventional disposable gelled electrodes. Results show high similarity in terms of noise amplitude and electrode-skin impedance between the conventional and textile electrodes with the addition of solid hydrogel or saline solution. Furthermore, we compared the shape of the electrically induced sEMG, as detected by conventional and textile electrodes from tibialis anterior. The comparison yielded an  $R^2$  value higher than 97% for all measurement conditions. Preliminary tests in dynamic conditions (walking) revealed the exploitability of the proposed electrode technology with saline application for the monitoring of sEMG for up to 35 min of activity. These results suggest that the proposed screen-printed textile electrodes may be an effective alternative to the conventional gelled electrodes for sEMG acquisition, thereby providing new opportunities in clinical and wellness fields.

**Index Terms**—Surface EMG, textile electrodes, screen-printing, M-wave.

Manuscript received December 5, 2018; revised March 19, 2019; accepted March 27, 2019. Date of publication May 23, 2019; date of current version July 4, 2019. This work has been carried out in the framework of the DoMoMEA Project, funded by Sardegna Ricerche with POR FESR 2014/2020 funds, Priority Axis I “Scientific Research, Technological Development and Innovation” and of the CONVERGENCE Project, funded by the ERA-NET—a H2020 Instrument. (Corresponding author: D. Pani.)

D. Pani, A. Spanu, and A. Bonfiglio are with the Department of Electrical and Electronic Engineering, University of Cagliari, 09123 Cagliari, Italy (e-mail: pani@diee.unca.it).

A. Achilli is with the Department of Electrical and Electronic Engineering, University of Cagliari, 09123 Cagliari, Italy, and also with the Department of Informatics, Bioengineering, Robotics and System Engineering, University of Genoa, 16145 Genoa, Italy.

M. Gazzoni and A. Botter are with LISiN, Department of Electronics and Telecommunications, Politecnico di Torino, 10129 Turin, Italy, and also with the PoliToBIOMed Lab, Politecnico di Torino, 10129 Turin, Italy. Digital Object Identifier 10.1109/TNSRE.2019.2916397

## I. INTRODUCTION

THE advent of smart textiles with sensing/actuation features and electronic components that can be integrated into garments has opened new avenues for physiological and environmental sensing. Moving on from the first steps taken in this field, as represented by the first examples of metallic wires embroidered or knitted with non-conductive fibers to produce conductive pads [1], [2], the industry has proposed smart garments for several applications. This has led to the commercial introduction of smart clothes for personal health and wellness, e.g., with the ability to detect electrocardiogram (ECG) signals [3], [4] or surface electromyogram (sEMG) signals [5], [6], or even to provide electrical stimulation for enhancing workouts [7]. As stated, these smart clothes use integrated textile electrodes by embedding metallic wires into the fabric. Although this solution is robust, in order to avoid the introduction of seamed electrodes, their production must be integrated into the main garment weaving process. The main goal of research in this field is to identify valid alternatives to the metal wires used in the production of these electrodes, and possibly limiting the impact on the garment fabrication process and achieving better performance [8]. Beyond an improvement of the technological process, avoiding the use of metallic electrodes would positively impact users’ comfort, especially in long-term measurements [9], [10]. This could be a crucial aspect in specific sEMG applications such as the production of electrodes for sEMG-controlled prostheses [11].

A variety of sEMG electrodes specifically designed to be integrated into clothes has been proposed in the last few years. These electrodes enable the acquisition of sEMG signals from several body regions: frontalis, temporalis and lateral rectus [12], vastus lateralis, rectus femoris and vastus medialis [13], gluteals, vasti, hamstrings [14], masticatory muscles [15], trapezius muscle to monitor stress load [16], and flexor and extensor forearm muscles [17].

In all these works, the electrodes were composed of metallic elements either added onto finished clothes in the form of conductive patches or wires or integrated as screen-printed electrodes deposited onto a plastic substrate. When embedding external electrodes in clothes, both solutions can affect the roughness of the surface and, ultimately, the comfort of the wearer.

This work presents the validation of the performance of seamless screen-printed polymer-based textile electrodes in sEMG signal detection. We functionalized a pure cotton fabric by the deposition of poly-3,4-ethylenedioxythiophene doped

with poly(styrene sulfonate) (PEDOT:PSS). Deposition by screen-printing changes the chemo-physical properties of the textile substrate without affecting its mechanical features, which is essential for obtaining textile electrodes characterized by high wearer-comfort levels. We assessed the performance of these sEMG electrodes on the tibialis anterior muscle in different conditions, namely with or without the presence of an electrolyte between electrode and skin, by recording the muscular activity induced by electrical stimulation. We chose this configuration to reduce the physiological variability of voluntary muscular contraction, thus allowing a fine comparison of the signal morphology. We evaluated both the effect of the electrode area and the presence or absence of electrolytes. We then compared the results with those of a conventional disposable gelled Ag/AgCl electrode of the same size, which are clearly not adequate for the development of smart garments but represent the gold standard for physiological biopotential recordings on the human body. Even though a complete assessment of the textile electrode performance in dynamic conditions is beyond the scope of this work, a preliminary investigation was also performed to evaluate the feasibility of the application of the proposed technology in rehabilitation contexts, where the tasks are often dynamic.

## II. MATERIAL AND METHODS

In this study, we produced screen-printed textile electrodes printed on a 100% cotton fabric and compared their performances with those of disposable gelled Ag/AgCl electrodes. The textile electrode production process is based on a standard fabric screen-printing procedure, and uses a conductive ink composed of HERAUS CLEVIOUS<sup>TH</sup> PH1000 PEDOT:PSS, ethylene glycol and GOPS, as described in a previous work related to ECG signal acquisition [18]. After deposition on the textile substrate, we dried the ink by placing the electrodes in an oven for 15 minutes at 70 °C. For the deposition, we used a 43T mesh with a mask containing two different geometries. The first geometry ( $\varnothing 24$ ) combines a round shape 24 mm in diameter and a rectangular path (5 mm  $\times$  15 mm), and the second ( $\varnothing 10$ ) uses the same rectangular path and a 10-mm-diameter round shape (Fig. 1, bottom panel). We added the rectangular path to the electrodes as a way to acquire the signal through a crocodile connection clipped directly onto the fabric (for static recordings) or through a snap-on button directly crimped on the fabric and isolated from the skin (for dynamic recordings).

### A. Electrodes Characterization in Static Conditions

To validate the performance of the electrodes in detecting sEMG signals, we analyzed both the electrical parameters and the sEMG signal characteristics they detected.

We evaluated the performance of the screen-printed electrodes in three different conditions: i) dry, ii) after the addition of a few drops of saline solution (0.9%) to the electrode surface, and iii) with a solid KCl hydrogel layer (Spes Medica Srl, Genoa, Italy) applied to the electrode surface.

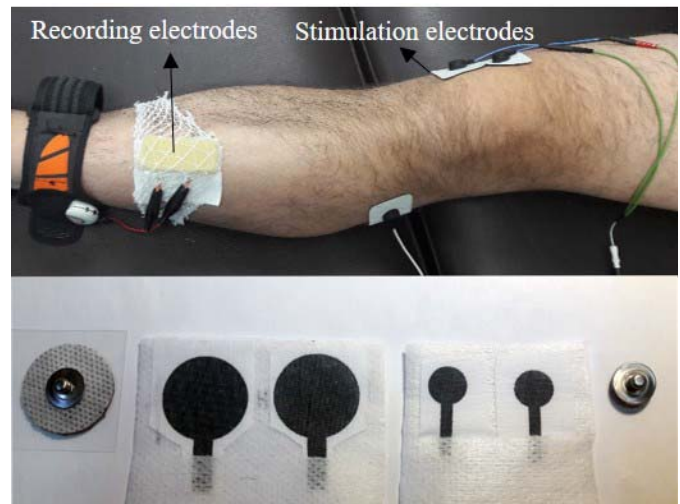


Fig. 1. From top to bottom: measurement setup and the electrodes (from left to right: 24 mm gelled Ag/AgCl electrodes,  $\varnothing 24$  and  $\varnothing 10$  textile electrode pairs, and 10mm reduced gelled Ag/AgCl electrodes).

Dry condition represents the ideal situation of a wear-and-play smart garment. However, dry electrodes present several limitations mainly ascribable to the skin-electrode interface. By adding saline, which is a weak electrolyte, we can promote the reactions at the interface but also increase the active surface of the electrode by filling the recessed parts of its rough surface [8]. Remarkably, saline emulates sweat because of the presence of NaCl in a similar percentage (0.1% to 0.4% [19]). Its presence could be substituted by tap water with similar results [20], thus supporting the idea that a better adhesion to the skin of the wet fabric is actually important [21]. Lastly, hydrogel was tested to have a closer comparison with disposable commercial electrodes [22]. In this case, the ionic concentration is typically higher, if compared to that of saline, and the adhesion with the skin is maximized by the adhesive nature of the material, improving the contact stability [21], [23]. Nevertheless, the most important conditions are represented by dry and wet electrodes, which fit better the needs of smart garments.

We compared the results with those obtained using standard gelled Ag/AgCl electrodes (CDES000024 by Spes Medica Srl, Genoa, Italy). To ensure a like-with-like comparison, we used Ag/AgCl electrodes with a nominal diameter of 24 mm and with a reduced diameter of 10 mm, which we obtained by cutting them with a hollow cutter punch (Fig. 1). This choice maximizes the similarity between the proposed textile and commercial electrodes. The hydrogel added to our textile electrodes was also the same as that used with the commercial Ag/AgCl electrodes.

The study population consisted of ten healthy volunteer subjects. The study was performed following the principles outlined in the Helsinki Declaration of 1975, as revised in 2000. Institutional review board approval was obtained from ASL 1 Torino, Italy, Prot. n. 0010610. All subjects signed an informed consent regarding data acquisition and use prior to their participation in the recording protocol.

We characterized the electrode performance on the tibialis anterior while the subject was resting on an examination couch in a semi-sitting position. Before electrode placement, we shaved the skin and gently applied a skin preparation gel (NuPrep, by Weaver, Colorado, USA).

For each measurement, we applied two separate screen-printed textile electrodes to the skin using medical tape, with a distance between their centers equal to 30 mm for the 24-mm electrodes and 22 mm for the 10-mm ones. Electrode separation prevents any direct conductive path through the fabric when the saline solution is added. We placed a layer of foam (5-mm thick) over both electrodes and secured it in place using a tubular net bandage to enhance fabric adhesion onto the skin [24] and to maintain a stable and continuous pressure [25] and skin humidity [26] during measurement (see Fig. 1). The same positioning was used during testing of the commercial electrode.

**1) Electrical Parameters Analysis:** First, we analyzed the surface conductivity of the screen-printed textile electrodes. For this purpose, we measured the sheet resistance of the functionalized textile substrates using the four-probe method.

Next, we measured the electrode-skin impedance, which is an important parameter that can act as reference when comparing other figures of merit such as noise or signal amplitude. We measured the impedance with a custom-made impedance meter (LISiN, Politecnico di Torino, Italy). This device converts a sinusoidal voltage input into a proportional current signal (200 nA peak-to-peak amplitude) and measures the voltage drop between the electrodes tested. Using a Matlab routine, we computed the impedance module as the amplitude ratio between the measured voltage and injected current, for a frequency sweep in the range 10–1,000 Hz. For each measure, we extrapolated the impedance value at 50 Hz from the experimental dataset for comparison of the experimental conditions.

To quantify the noise contribution associated with the whole setup, we performed a signal acquisition with the subjects at rest, while making no voluntary or induced muscular activation on the tibialis anterior.

To do so, we used a DuePro amplifier (OT Bioelettronica, Torino, Italy; sampling frequency: 2048 Hz, bandwidth 10–500 Hz, A/D: 16-bit). During the measurement, we inserted the DuePro device into an armband fastened close to the ankle in proximity to the electrodes to minimize the wire lengths, movements, and electrode traction. To display and record the signals, we connected the amplifier via Bluetooth to a host PC running a custom-made acquisition software (LISiN, Politecnico di Torino, Torino, Italy).

We band-pass filtered the detected signal in the 10–500 Hz frequency band and removed any power-line interference using a spectral interpolation technique [27]. We then obtained noise estimations by calculating the *rms* of the filtered signal over a 10 s window and validated the results by evaluating the same parameter during a quiescent period in the stimulation protocol. From the same 10 s segments used in the *rms* estimations, we also estimated the power spectral density (PSD) of the noise using Welch's method with 4 s windows (1-s overlap). We performed this analysis for each subject in the typical

range of the sEMG signal, i.e., from 10 Hz to 500 Hz [28]. We used box plots to represent the skin-electrode impedance and *rms* of the noise distributions. In these plots, the median is highlighted, the box defines 50% of the samples between the first and third quartile, and the whiskers range from the minimum to maximum value, excluding outliers (represented separately). Outliers are defined as data values larger than  $q3 + 1.5(q3 - q1)$  or smaller than  $q1 - 1.5(q3 - q1)$ , where  $q1$  and  $q3$  are the 25<sup>th</sup> and 75<sup>th</sup> percentiles, respectively, which correspond to approximately  $\pm 2.7 \sigma$  and 99.3% coverage, if the data were normally distributed.

We statistically analyzed the skin-electrode impedance and *rms* of the noise, at rest, by aggregating the results from all the subjects testing the same electrode and comparing the populations in pairs (Ag/AgCl electrodes against textile electrodes of the same size, in different conditions). First, we performed a Kolmogorov–Smirnov normality test of the subject distributions to choose the most appropriate statistical analysis method, i.e., the Student's t-test or the nonparametric Mann–Whitney U test, depending on whether the distributions were normally distributed or not, respectively. Statistical significance is considered to be  $p < 0.05$ .

**2) sEMG Signal Analysis:** Due to the large variability in the interferential sEMG patterns generated by voluntary muscular contractions, the approach we followed in this work is similar to that described in [29], which is based on the analysis of the electrically-induced sEMG response, i.e. the M-wave. In electrically-induced contractions, the number of activated motor units, and therefore the shape of the induced M-wave, depends primarily on the stimulation amplitude and on the position of the stimulating electrodes [30]. Both parameters were kept constant across trials on the same subjects. In this condition, the most relevant source of variability influencing the M-wave shape is the electrode-skin interface, which in turn depends on the skin characteristics and electrode type, but not on the considered muscle. For this reason, for sEMG analysis in static conditions, only one muscle was considered, and we adopted the same setup described above to record the noise. We used a DS7AH electrical stimulator (Digitimer Ltd, UK) to stimulate the branch of the peroneal nerve that innervates the tibialis anterior via two disposable stimulation gelled electrodes (bipolar nerve stimulation).

We configured the stimulator to generate stimulation pulses with 300  $\mu$ s duration at 2 Hz. For each subject, at the beginning of the experiment, we identified the stimulation amplitude that induced a maximal M-wave and kept it constant throughout all the experimental conditions (i.e. different, tested electrodes). The average current value used for the stimulation was  $24 \pm 5$  mA.

For each subject, electrode, and condition, we performed the analysis on a prototypical M-wave obtained by averaging of ten M-waves that occurred during that recording. We adopted this averaging procedure to reduce the effect of any possible, subtle variability in the physiological responses to the electrical stimulation [31]. Using this process, it was possible to compare each signal acquired by the textile electrodes with that acquired by the disposable gelled Ag/AgCl electrodes of the same size placed in the same position. We determined



the similarity of the M-wave templates obtained from the textile and commercial electrodes. To do so, we produced a scatter plot of the individual samples of the two synchronized M-wave templates (one against the other), and computed three parameters: slope,  $R^2$ , and mean square error normalized by the energy of the M-wave template obtained from the reference Ag/AgCl electrodes (NMSE) [29]. For these parameters, we obtained descriptive statistics using mean and standard deviation, in consideration of the physiological differences between subjects in the different recordings.

### B. Testing Textile Electrodes During a Dynamic Task

The experimental protocol described in Section A was designed to characterize the interface between different electrode types and the skin in terms of impedance, noise and quality of detected sEMG. In order to isolate the effect of the electrode on the measured variables, these measures were performed in well-controlled and standardized experimental conditions; static and electrically-induced contractions. In this section, we describe a preliminary set of measurements aimed at demonstrating the feasibility of sEMG acquisitions also in dynamic contractions, a condition more similar to those occurring in applied contexts, where the implementation of this electrode technology could be more useful.

Surface EMG signals were acquired (DuePro amplifier, OT Bioelettronica, Torino, Italy) from medial gastrocnemius (MG) and tibialis anterior (TA) in three healthy subjects during walking. For each muscle, a pair of textile electrodes ( $\varnothing 24$ ) were positioned beside a pair of Ag/AgCl electrodes. For both electrode types, the inter-electrode distance was 25 mm. Before textile electrodes positioning, the electrode surface was dampened with two drops of saline solution. As for the static contractions, we placed a layer of foam (5 mm thick) over the back of both textile electrodes and then we secured this textile stack in place using a lycra sleeve (the electrodes were then not fixed on the sleeve). The experimental protocol consisted in ten walking trials of 20 steps each. Subjects were asked to walk at the preferred velocity and consecutive trials were separated by 5 minutes of rest. For each trial, sEMG envelopes of TA and MG were segmented using the heel-strikes instants obtained from a footswitch (Biometrics Ltd, UK) positioned under the right heel. The cross-correlation between the synchronized averaging of the sEMG envelopes detected by textile electrodes and by Ag/AgCl electrodes was then computed to quantify the differences between signals recorded with the two types of electrodes. The time course of cross-correlation values provided a description of the effect of time on the quality of sEMG recorded by textile electrodes, under the assumption that the Ag/AgCl electrode contact remained unchanged throughout the experiment.

## III. RESULTS

The sheet resistance was  $390 \pm 60 \Omega/\text{sq.}$  and  $410 \pm 150 \Omega/\text{sq.}$ , respectively, for the  $\varnothing 24$  and  $\varnothing 10$  electrodes.

Figure 2 shows box plots of the skin-electrode impedance measured in different conditions by the screen-printed and gelled electrodes. The results of the Kolmogorov–Smirnov test

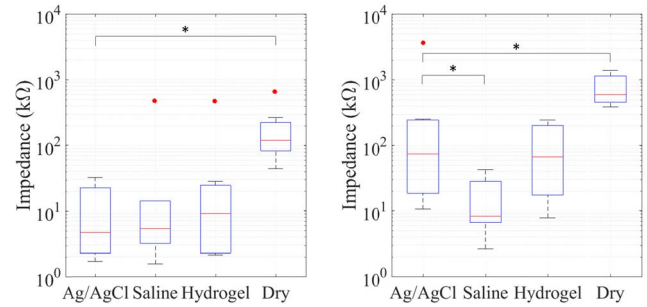


Fig. 2. Box plot of the skin-electrode impedance for each electrode size and measurement condition (from left to right, for  $\varnothing 24$  and  $\varnothing 10$ ).

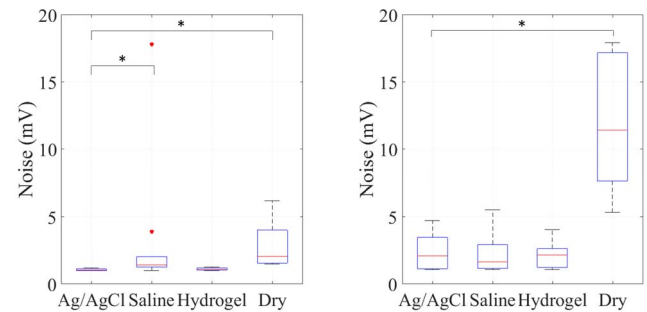


Fig. 3. Box plot of the *rms* of the noise for each electrode size and measurement condition (from left to right, for  $\varnothing 24$  and  $\varnothing 10$ ).

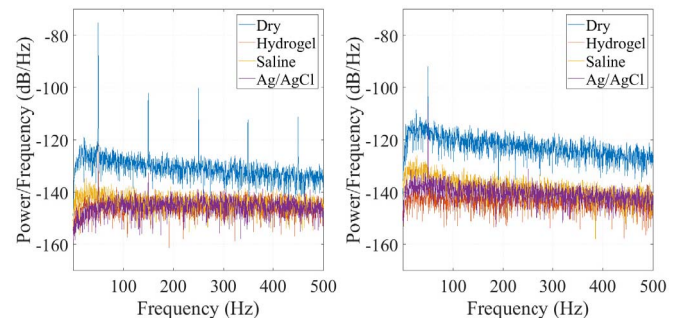


Fig. 4. PSD of the noise for each electrode and condition (from left to right, for  $\varnothing 24$  and  $\varnothing 10$ ).

on these skin-electrode impedance populations suggested the adoption of the U test. This test revealed a significant statistical difference between the disposable gelled Ag/AgCl electrodes and dry textile electrodes of any size ( $p < 0.002$ ), and also for the  $\varnothing 10$  electrodes with saline ( $p = 0.0036$ ). Conversely, we found no statistically significant difference in the other cases ( $\varnothing 24$  and  $\varnothing 10$  with hydrogel,  $p > 0.7$  and  $\varnothing 24$  with saline,  $p = 0.97$ ). Figure 3 shows the *rms* of the signal at rest (noise) for all the electrode conditions. Figure 4 shows the Welch's PSDs of these signals for a single subject in each recording. We also obtained the same behavior observed at rest during the stimulation protocol in the quiescent regions of the sEMG signals.

The results of the Kolmogorov–Smirnov test on these noise populations again suggested the adoption of the U test, since the distributions were not normal. This test also revealed a

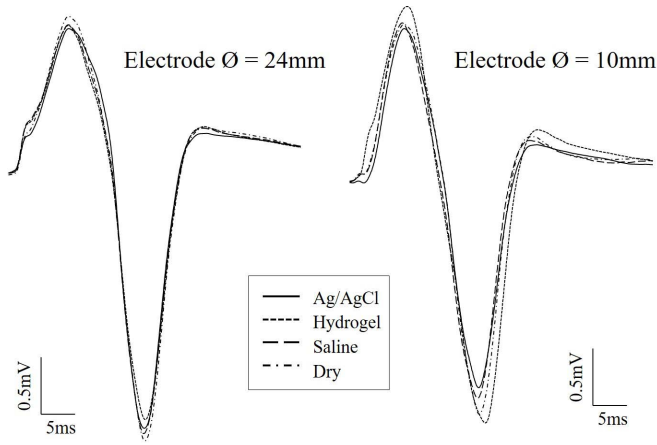


Fig. 5. Average M-waves acquired on the same subject with the different electrodes in different measurement conditions (from left to right, for  $\varnothing 24$  and  $\varnothing 10$ ).

TABLE I

COMPARISON OF TEXTILE AND COMMERCIAL ELECTRODES IN TERMS OF LINEAR REGRESSION PARAMETERS (MEAN  $\pm$  STD OVER 10 SUBJECTS)

| $\varnothing 24$ electrodes |          |                 | $\varnothing 10$ electrodes |          |                 |
|-----------------------------|----------|-----------------|-----------------------------|----------|-----------------|
| NMSE %                      | Dry      | 3 $\pm$ 2       | NMSE %                      | Dry      | 4 $\pm$ 3       |
|                             | Saline   | 2 $\pm$ 1       |                             | Saline   | 5 $\pm$ 2       |
|                             | Hydrogel | 2 $\pm$ 1       |                             | Hydrogel | 4 $\pm$ 3       |
| SLOPE mV/mV                 | Dry      | 1.05 $\pm$ 0.09 | SLOPE mV/mV                 | Dry      | 1.06 $\pm$ 0.12 |
|                             | Saline   | 0.98 $\pm$ 0.09 |                             | Saline   | 1.00 $\pm$ 0.12 |
|                             | Hydrogel | 0.98 $\pm$ 0.07 |                             | Hydrogel | 1.09 $\pm$ 0.08 |
| R <sup>2</sup>              | Dry      | 0.98 $\pm$ 0.01 | R <sup>2</sup>              | Dry      | 0.98 $\pm$ 0.01 |
|                             | Saline   | 0.98 $\pm$ 0.01 |                             | Saline   | 0.97 $\pm$ 0.02 |
|                             | Hydrogel | 0.99 $\pm$ 0.01 |                             | Hydrogel | 0.98 $\pm$ 0.01 |

significant statistical difference between the disposable gelled Ag/AgCl electrodes and the dry textile electrodes of any size ( $p < 0.0002$ ), as well as for the  $\varnothing 24$  electrodes with saline ( $p = 0.0028$ ). Conversely, we found no statistically significant difference in the other cases ( $\varnothing 24$  and  $\varnothing 10$  with hydrogel,  $p > 0.10$  and  $p > 0.85$  respectively, and  $\varnothing 10$  with saline,  $p > 0.97$ ).

During electrical stimulation, we computed the average M-wave per each electrode in each recording condition. Figure 5 shows two examples of the average M-waves obtained on the same subject with all the electrodes tested in this experiment, considering different measurement conditions for the textile electrodes.

Figure 6 shows the linear regression model adopted to compute the parameters for comparison of the disposable gelled Ag/AgCl electrodes with their textile counterpart, for a single subject and the larger electrode size ( $\varnothing 24$ ). Table I lists the average parameters obtained from the linear regression, along with their errors, as expressed by standard deviation, for the ten subjects.

Figure 7 reports the results of the analysis on sEMG signals detected during walking for one representative subject.

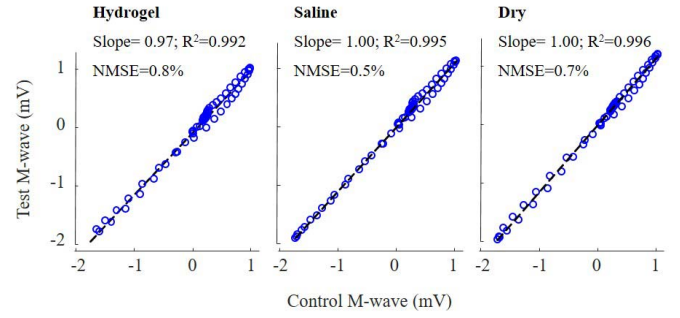


Fig. 6. Linear regression between average M-waves recorded with disposable gelled Ag/AgCl electrodes (control M-wave) and with the screen-printed textile electrodes, in different conditions (test M-wave). These plots refer to a single subject, for the  $\varnothing 24$  electrodes.

The upper panel (Fig. 7a) shows the quality of raw sEMG signals detected from MG and TA by Ag/AgCl and textile electrodes. Signals of five steps for the first end eighth trial (corresponding to 0 and 35 minutes from the electrodes application) are depicted. The signal quality of the two electrodes type is comparable for the first trial, while it is remarkably different for the eighth trial, where the signals detected from textile electrodes are affected by low frequency artifacts. The presence of these artifacts affects the shape of the signal envelope, which is shown for MG in Fig. 7b. As compared with the envelope of the first trial, that of trial 8 is comparable for Ag/AgCl electrodes, while it is highly distorted for textile electrodes. This behavior was quantified for the two muscles with the cross-correlation between sEMG envelopes detected by Ag/AgCl and Textile electrodes (Fig. 7c). The graph in Fig. 7c depicts a slow, though progressive, decrease of the cross-correlation, which becomes faster after 30 minutes from the electrodes positioning. For both muscles and for all the subjects, the cross-correlation was larger than 0.95 for the first trial and decayed below the threshold of 0.85 after 35, 35 and NN minutes for MG and 45, 40, 50 minutes for TA (where NN means the cross-correlation was always above the threshold for our observation time: 45 min).

#### IV. DISCUSSION

The sheet resistance results highlight the high repeatability of the screen-printing technique used to fabricate the textile electrodes by screen-printing, thus demonstrating the high reproducibility of the printing process, due to the possibility of precisely controlling the amount of ink that is deposited on the substrate [18].

However, for the detection of physiological signals, sheet resistance is not the only parameter involved in electrode performance [8]. Other aspects, such as the skin-electrode impedance, affect the quality of conductive materials used as biopotential electrodes.

The skin-electrode impedance measured before each sEMG measurement can be used to describe how electrode size and electrolytes influence performance [7]. In the signal acquisition without any electrolyte, the impedance value was high even if a mild skin treatment had been applied after shaving. The box plots in Fig. 2 clearly indicate that the presence of the

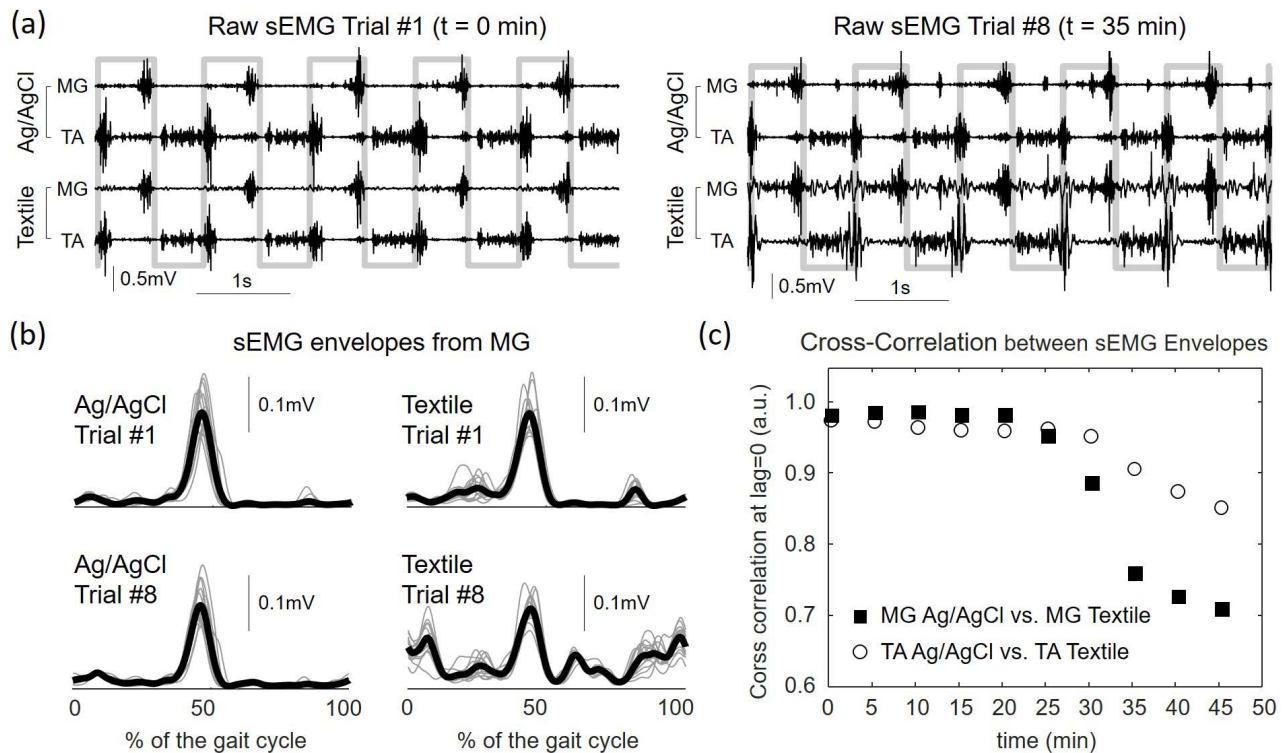


**Fig. 7.** (a) Raw sEMG signals detected by Ag/AgCl and textile electrodes during five gait cycles for the first and eighth trials. The thick, gray trace is the signal from the footswitch positioned under the right heel. (b) sEMG envelopes detected in MG from Ag/AgCl and textile electrodes during trials 1 and 8. Grey traces are the envelopes corresponding to each step, the black signal is the average envelope. (c) Time course of the cross-correlation between sEMG envelopes detected by the two electrode types. Data from ten trials recorded with five-minute rest between consecutive trials are reported.

electrolyte influenced this parameter for both the  $\varnothing 10$  and  $\varnothing 24$  textile electrodes, in both cases contributing to decreasing the skin-electrode impedance by an order of magnitude. Thus, no statistically significant difference was found between the conventional and textile electrodes in the presence of an electrolyte. According to the scientific literature [32], there is also an inverse relationship between the electrode size and the skin-electrode impedance, regardless of the measurement condition.

A similar analysis of the *rms* of the noise with the  $\varnothing 24$  and  $\varnothing 10$  electrodes leads to a similar conclusion. The first aspect is the noise level in dry conditions, which reaches, respectively,  $3 \pm 2 \mu\text{V}$  and  $12 \pm 5 \mu\text{V}$  for the two textile electrode sizes. The box plot of the noise indicates that, in this case, the addition of electrolytes also dramatically improves the electrode performance, leading to values comparable to those of conventional electrodes.

Overall, the addition of a saline solution introduces greater variability, compared to a solid hydrogel, and this is reflected by the presence of outliers. This variability is probably due to transient instability of the contact caused by the limited adhesion of the electrodes to the skin [25]. The statistical analysis results again reveal the substantial similarity in the electrode performances when an electrolyte is used, at least when the electrodes are not small.

A comparative analysis of Figs. 2 and 3 shows similarity, being the two aspects dependent, at least in principle. To analyze such a dependency, we studied the data leading to

the boxplots in Figs. 2 and 3, by considering each electrode size and type/condition separately. We computed the Pearson's correlation coefficient and the Spearman's rank correlation between the variables *rms* of the noise and impedance. The former test can only reveal linear dependency between the two parameters, and then a proportionality of the centered observations, whereas the latter looks at non-linear dependency of the data leading to a monotonic function (similar rank of the two parameters). By averaging the correlation coefficients over the two sizes, which present a similar behavior (data not shown), for each electrode type/condition, we obtained that noise and impedance are highly correlated for all the electrodes but the textile with saline one. In detail, Ag/AgCl electrodes reported 0.81 (Pearson) and 0.91 (Spearman), which are similar to those obtained for the dry textile electrodes (0.87 and 0.90, respectively) and for the textile electrodes with solid hydrogel (0.93 and 0.97, respectively). Conversely, we obtained very low correlation coefficient values for the textile electrodes with saline solution ( $-0.24$  and  $-0.10$ , respectively for Pearson and Spearman), which confirms that the noise in this case is mainly due to the movement artifacts (low-frequency) associated to the limited electrode stability on the skin rather than to the amplification of the common-mode due to the skin-electrode impedance imbalance between the couple of recording electrodes [33], typically experienced when a high skin-electrode impedance is present.

All these considerations were confirmed by the PSD results, which reveal that dry electrodes experience a generally higher



noise level and power-line interference harmonics, mainly due to the higher skin-electrode impedance, also leading to an attenuation of the signal of interest. Furthermore, the PSD reveals that most of the noise for the textile electrodes with saline solution occurs in the lowest part of the spectrum, confirming the previous considerations. In fact, from Fig. 4 it is also clear how the adhesive electrolyte (present in disposable gelled electrodes and in the textile with solid hydrogel) operates on the low frequencies by reducing the baseline wandering typical of textile electrodes and due to a loose contact [25] and to the material characteristics [20]. Remarkably, the PSD at rest for the proposed textile electrodes composed of organic polymers, except in dry conditions, is comparable with that in other works wherein the EMG signal was acquired with electrodes composed of metallic wires in contact with the skin [34]. The results of the M-wave analysis on the ten volunteers, as reported in Table I, indicates that the signal acquired in dry conditions is less similar to those acquired using conventional electrodes or by adding some electrolyte to the textile electrodes. We computed the NMSE,  $R^2$ , and slope values from the linear correlations between the average M-waves recorded using conventional electrodes and those recorded using the screen-printed electrodes. The descriptive statistics in Table I reveal a similar behavior of electrodes produced using different technologies in every condition, independent of electrode size. Remarkably, both the  $R^2$  coefficient close to one and the average slope of around 1 mV/mV indicate high similarity between the M-waves curves detected by the textile and gelled Ag/AgCl electrodes.

In this study, the analysis of sEMG signals during a walking task was included as feasibility proof of the acquisition in dynamic contractions. Although from a limited subject population, the results of this analysis show somehow consistent indications on the quality and the usability time of these electrodes. Indeed, for both the muscles of the three subjects tested, the quality of sEMG signals remained adequate (limited motion artifacts and cross-correlation with a reference envelope greater than 0.85) for at least 30 minutes. The reasons for the signal quality reduction were likely attributable to both the electrode drying, which leads to a worsening of the electrode-skin interface properties, as demonstrated in the comparison between different electrodes (Fig. 2 and 3), and the creasing of the cotton fabric, which was not fixed to the elastic sleeve. This interpretation is supported by the evidence that all the textile electrodes were dry at the time we removed them, 45 min after their application, and at least one of them was clearly creased. An in-depth analysis of the performance of the proposed textile electrodes in dynamic contractions would then require a larger population and a larger set of controlled dynamic tasks and conditions, and the direct printing on the elastic sleeve of the electrodes to avoid creasing of the electrode substrate. Remarkably, if only the electrode drying process remains to hamper a stable-quality signal acquisition, moisturizing the electrodes repeatedly over time from the outside of the garment by saline solution is an easy way to solve of this problem [35]. Furthermore, saline emulates sweat that could take place during physical activity due to transpiration [21], so that in some cases exogenous wetting

of the electrode could be avoided. Overall, these preliminary results demonstrate the feasibility of the proposed technology as a way to functionalize common fabrics to obtain sEMG electrodes of adequate quality.

## V. CONCLUSIONS

In this work, we presented an in-depth characterization of the performance of polymer-based textile electrodes in sEMG signal acquisition. The experimental results suggest that these electrodes can be used in static conditions to study the sEMG signal in the presence of a liquid or solid electrolyte (such as saline or solid hydrogel), without significant differences in the performance from that of conventional disposable gelled sEMG electrodes. This is important because the wet condition is similar to the one achievable during physical exercise, when sweating occurs, or, when the activity is less intense as for rehabilitation, it can be easily obtained by periodically wetting the external surface of the garment with saline and letting the liquid able to reach the active area of the electrode. However, the use of the electrodes in dry conditions is limited by a higher noise level, which slightly affects the M-wave morphology, but may be more problematic on lower-amplitude sEMG signals, such as those acquired from voluntary contractions. In light of the results obtained for both large and small electrodes, this technology may be adopted to design bipolar or multichannel electrodes for applications requiring high electrode conformability and simple setups. On the way paved by the results presented in this work, more extensive trials in dynamic conditions are being carried out for the complete characterization of these electrodes for sEMG applications.

## REFERENCES

- [1] M. Stoppa and A. Chiolerio, "Wearable electronics and smart textiles: A critical review," *Sensors*, vol. 14, no. 7, pp. 11957–11992, Jul. 2014.
- [2] C. Gonçalves, A. F. da Silva, J. Gomes, and R. Simoes, "Wearable E-textile technologies: A review on sensors, actuators and control elements," *Inventions*, vol. 3, no. 1, p. 14, 2018.
- [3] J.-A. Park, H.-J. Han, J.-C. Heo, and J.-H. Lee, "Computer aided diagnosis sensor integrated outdoor shirts for real time heart disease monitoring," *Comput. Assist. Surg.*, vol. 22, pp. 176–185, Oct. 2017.
- [4] J. Wang, C.-C. Lin, Y.-S. Yu, and T.-C. Yu, "Wireless sensor-based smart-clothing platform for ECG monitoring," *Comput. Math. Methods Med.*, vol. 2015, Oct. 2015, Art. no. 295704.
- [5] S. L. Colyer and P. M. McGuigan, "Textile electrodes embedded in clothing: A practical alternative to traditional surface electromyography when assessing muscle excitation during functional movements," *J. Sports Sci. Med.*, vol. 17, no. 1, pp. 101–109, Mar. 2018.
- [6] C. Pylatiuk *et al.*, "Comparison of surface EMG monitoring electrodes for long-term use in rehabilitation device control," in *Proc. IEEE Int. Conf. Rehabil. Robot.*, Jun. 2009, pp. 300–304.
- [7] H. Zhou *et al.*, "Stimulating the comfort of textile electrodes in wearable neuromuscular electrical stimulation," *Sensors*, vol. 15, no. 7, pp. 17241–17257, Jul. 2015.
- [8] D. Pani, A. Achilli, and A. Bonfiglio, "Survey on textile electrode technologies for electrocardiographic (ECG) monitoring, from metal wires to polymers," *Adv. Mater. Technol.*, vol. 3, no. 10, Oct. 2018, Art. no. 1800008.
- [9] G. Li, Y. Geng, D. Tao, and P. Zhou, "Performance of electromyography recorded using textile electrodes in classifying arm movements," in *Proc. Annu. Int. Conf. IEEE Eng. Med. Biol. Soc. (EMBS)*, Aug./Sep. 2011, pp. 4243–4246.
- [10] A. Mangezi, A. Rosendo, M. Howard, and R. Stopforth, "Embroidered archimedean spiral electrodes for contactless prosthetic control," in *Proc. Int. Conf. Rehabil. Robot. (ICORR)*, Jul. 2017, pp. 1343–1348.



- [11] H. Zhang, L. Tian, L. Zhang, and G. Li, "Using textile electrode EMG for prosthetic movement identification in transradial amputees," in *Proc. IEEE Int. Conf. Body Sensor Netw. (BSN)*, May 2013, pp. 1–5.
- [12] G. M. Paul, F. Cao, R. Torah, K. Yang, S. Beeby, and J. Tudor, "A smart textile based facial EMG and EOG computer interface," *IEEE Sensors J.*, vol. 14, no. 2, pp. 393–400, Feb. 2014.
- [13] T. Finni, M. Hu, P. Kettunen, T. Vilavuo, and S. Cheng, "Measurement of EMG activity with textile electrodes embedded into clothing," *Physiol. Meas.*, vol. 28, no. 11, pp. 1405–1419, Nov. 2007.
- [14] P. Bifulco, M. Cesarelli, A. Fratini, M. Ruffo, G. Pasquariello, and G. Gargiulo, "A wearable device for recording of biopotentials and body movements," in *Proc. IEEE Int. Symp. Med. Meas. Appl.*, May 2011, pp. 469–472.
- [15] A. Nijima, T. Isezaki, R. Aoki, T. Watanabe, and T. Yamada, "hitoeCap: Wearable EMG sensor for monitoring masticatory muscles with PEDOT-PSS textile electrodes," in *Proc. ACM Int. Symp. Wearable Comput.*, Sep. 2017, pp. 215–220.
- [16] J. Taelman, T. Adriaensen, C. Van Der Horst, T. Linz, and A. Spaepen, "Textile integrated contactless EMG sensing for stress analysis," in *Proc. 29th Annu. Int. Conf. IEEE Eng. Med. Biol. Soc.*, Aug. 2007, pp. 3966–3969.
- [17] A. Shafit, R. B. R. Manero, A. M. Borg, K. Althoefer, and M. J. Howard, "Designing embroidered electrodes for wearable surface electromyography," in *Proc. IEEE Int. Conf. Robot. Automat. (ICRA)*, May 2016, pp. 172–177.
- [18] A. Achilli, A. Bonfiglio, and D. Pani, "Design and characterization of screen-printed textile electrodes for ECG monitoring," *IEEE Sensors J.*, vol. 18, no. 10, pp. 4097–4107, May 2018.
- [19] J. P. Reilly, *Applied Bioelectricity*. New York, NY, USA: Springer, 2011.
- [20] V. Marozas, A. Petrenas, S. Daukantas, and A. Lukosevicius, "A comparison of conductive textile-based and silver/silver chloride gel electrodes in exercise electrocardiogram recordings," *J. Electrocardiol.*, vol. 44, no. 2, pp. 189–194, Mar./Apr. 2011.
- [21] R. Paradiso, G. Loriga, N. Taccini, A. Gemignani, and B. Ghelarducci, "Wealthy—A wearable healthcare system: New frontier on e-textile," *J. Telecommun. Inf. Technol.*, vol. 4, pp. 105–113, 2005.
- [22] A. Achilli, D. Pani, and A. Bonfiglio, "Characterization of screen-printed textile electrodes based on conductive polymer for ECG acquisition," in *Proc. Comput. Cardiol. (CinC)*, vol. 44, Sep. 2017, pp. 1–4.
- [23] R. Paradiso, G. Loriga, and N. Taccini, "A wearable health care system based on knitted integrated sensors," *IEEE Trans. Inf. Technol. Biomed.*, vol. 9, no. 3, pp. 337–344, Sep. 2005.
- [24] D. Pani, A. Dessi, J. F. Saenz-Cogollo, G. Barabino, B. Fraboni, and A. Bonfiglio, "Fully textile, PEDOT: PSS based electrodes for wearable ECG monitoring systems," *IEEE Trans. Biomed. Eng.*, vol. 63, no. 3, pp. 540–549, Mar. 2016.
- [25] G. Paul, R. Torah, S. Beeby, and J. Tudor, "The development of screen printed conductive networks on textiles for biopotential monitoring applications," *Sens. Actuators A, Phys.*, vol. 206, pp. 35–41, Feb. 2014.
- [26] J. Löfhede, F. Seoane, and M. Thordstein, "Textile electrodes for EEG recording—A pilot study," *Sensors*, vol. 12, no. 12, pp. 16907–16919, Dec. 2012.
- [27] D. T. Mewett, K. J. Reynolds, and H. Nazeran, "Reducing power line interference in digitised electromyogram recordings by spectrum interpolation," *Med. Biol. Eng. Comput.*, vol. 42, no. 4, pp. 524–531, Jul. 2004.
- [28] E. Criswell, *Cram's Introduction to Surface Electromyography*. Burlington, MA, USA: Jones and Bartlett, 2011.
- [29] A. Botter, T. M. Vieira, I. D. Loram, R. Merletti, and E. F. Hodson-Tole, "A novel system of electrodes transparent to ultrasound for simultaneous detection of myoelectric activity and B-mode ultrasound images of skeletal muscles," *J. Appl. Physiol.*, vol. 115, no. 8, pp. 1203–1214, Oct. 2013.
- [30] R. Bonfiglioli *et al.*, "Usefulness of surface electromyography of hand muscles in the assessment of myoelectric parameters changes due to repetitive manual tasks," *Giornale Italiano Medicina Lavoro Ergonomia*, vol. 29, no. 3, pp. 575–578, Jul./Sep. 2007.
- [31] R. Merletti, M. Knaflitz, and C. J. DeLuca, "Electrically evoked myoelectric signals," *Crit. Rev. Biomed. Eng.*, vol. 19, no. 4, pp. 293–340, 1992.
- [32] G. Li, S. Wang, and Y. Y. Duan, "Towards gel-free electrodes: A systematic study of electrode-skin impedance," *Sens. Actuators B, Chem.*, vol. 241, pp. 1244–1255, Mar. 2017.
- [33] J. G. Webster, *Medical Instrumentation: Application and Design*, 4th ed. Hoboken, NJ, USA: Wiley, 2009.
- [34] T. Linz, L. Gourmelon, and G. Langereis, "Contactless EMG sensors embroidered onto textile," *4th Int. Workshop Wearable Implant. Body Sensor Netw. (BSN)*, 2007, pp. 29–34.